

The Inner Mitochondrial Membrane Has Aquaporin-8 Water Channels and Is Highly Permeable to Water*

Received for publication, December 17, 2004
Published, JBC Papers in Press, March 4, 2005, DOI 10.1074/jbc.C400595200

Giuseppe Calamita‡§, Domenico Ferri¶, Patrizia Gena‡, Giuseppa E. Liquori¶, Annie Cavalier||,
Daniel Thomas||, and Maria Svelto‡

From the ‡Dipartimento di Fisiologia Generale ed Ambientale and ¶Dipartimento di Zoologia, Laboratorio di Istologia e di Anatomia Comparata, Università degli Studi di Bari, 70126 Bari, Italy and the ||URA CNRS 256, Université de Rennes 1, Rennes, France

Mitochondria are remarkably plastic organelles constantly changing their shape to fulfil their various functional activities. Although the osmotic movement of water into and out of the mitochondrion is central for its morphology and activity, the molecular mechanisms and the pathways for water transport across the inner mitochondrial membrane (IMM), the main barrier for molecules moving into and out of the organelle, are completely unknown. Here, we show the presence of a member of the aquaporin family of water channels, AQP8, and demonstrate the strikingly high water permeability (P_f) characterizing the rat liver IMM. Immunoblotting, electron microscopy, and biophysical studies show that the largest mitochondria feature the highest AQP8 expression and IMM P_f . AQP8 was also found in the mitochondria of other organs, whereas no other known aquaporins were seen. The osmotic water transport of liver IMM was partially inhibited by the aquaporin blocker Hg²⁺, while the related activation energy remained low, suggesting the presence of a Hg²⁺-insensitive facilitated pathway in addition to AQP8. It is suggested that AQP8-mediated water transport may be particularly important for rapid expansions of mitochondrial volume such as those occurring during active oxidative phosphorylation and those following apoptotic signals.

Mitochondrial volume is of pivotal importance for the activity of the electron transport chain (1) and a control point of apoptosis (2). Changes in mitochondrial volume occur in many other physiological and patho-physiological conditions, including intracellular signal transduction, liver regeneration, ischemia/reperfusion-induced damage, and anoxia (3–5). Mitochondria are well behaved osmometers, and swelling and contraction of the mitochondrial matrix and related changes to mitochondrial morphology are the consequence of the water movement that osmotically accompanies the net transport of solutes into and out of the mitochondrion (6), respectively. Mitochondrial volume changes are modulated by the net move-

ment of solutes including K⁺ and Ca²⁺ ions across the IMM¹ (7, 8). The inner mitochondrial membrane acts as a major barrier for the solutes and water moving between the cytoplasm and the mitochondrial matrix, the outer membrane being freely permeable to molecules of up to 1.5 kDa due to the presence of the exceedingly large pores formed by VDAC, the voltage-dependent anion channel (9). However, although a number of IMM transport systems have been cloned and characterized for their ability to transport solutes across the IMM (10), the molecular pathway for the movement of water remains obscure. Important clues for understanding the molecular bases of the mitochondrial osmotic properties were recently provided by the identification of an aquaporin water channel (11), AQP8, in rat hepatocyte mitochondria (12). AQP8 was also found in intracellular vesicles that are shuttled to the hepatocyte apical membrane under choleretic stimuli such as those brought about by glucagon (13). This led us to hypothesize the existence of two distinct pools of AQP8 in hepatocytes, one involved in primary bile secretion and another related to intracellular osmoregulation (14). As AQP8 is predominantly expressed within the cell interior (12, 15) and displays a very distinct gene organization and evolutionary pathway (16, 17), we also suggested that AQP8 evolved separately to feature intracellular specializations lacking in other mammalian aquaporins (12).

To investigate possible correlations between mitochondrial AQP8 expression, and mitochondrial morphology and water permeability, we have now defined the biochemical and ultrastructural localization of AQP8 in the submitochondrial compartments, characterized the molecular pathways and biophysics of water transport across the IMM, and suggested functions for AQP8 in mitochondria.

MATERIALS AND METHODS

Subcellular and Submitochondrial Membrane Fractionations—Subcellular membranes were prepared from adult male Wistar rats weighing 250–300 g (Morini, S. Polo D'Enza, Italy). Rats were fed with a standard diet and water *ad libitum*. For all experiments, rats were decapitated after anesthesia, and livers and other organs were quickly removed and processed depending on the specific preparation. All experiments carried out were in accordance with the principles for research involving animals authorized by The University of Bari. For the isolation of subcellular membrane fractions, livers were homogenized with a Potter-Elvehjem homogenizer (four strokes in 1 min at 500 rpm) in an isolation medium consisting of 220 mM mannitol, 70 mM sucrose, 20 mM Tris-HCl, 1 mM EDTA, and 5 mM EGTA, pH 7.4. The homogenate was centrifuged at 500 × *g* for 10 min at 4 °C, and the pellet consisting of nuclei and unbroken cells was discarded; the resulting supernatant was centrifuged at 1,000 × *g* for 10 min at 4 °C and the related pellet

* This work was funded by FIRB (Fondo per gli Investimenti della Ricerca di Base, Grant RBAU01RANB; to G. C. and M. S.) and CEGBA (Centro di Eccellenza di Genomica in campo Biomedico ed Agrario; to G. C. and M. S.). The costs of publication of this article were defrayed in part by the payment of page charges. This article must therefore be hereby marked “advertisement” in accordance with 18 U.S.C. Section 1734 solely to indicate this fact.

§ To whom correspondence should be addressed: Dipartimento di Fisiologia Generale ed Ambientale, Università degli Studi di Bari, Via Amendola 165/A-70126 Bari, Italy. Tel.: 39-0805442928; Fax: 39-0805443388; E-mail: calamita@biologia.uniba.it.

¹ The abbreviations used are: IMM, inner mitochondrial membrane; AQP, aquaporin; OMM, outer mitochondrial membrane; PBS, phosphate-buffered saline.

($1,000 \times g$ membrane fraction) was washed twice before being resuspended in isolation medium to which a mixture of protease inhibitors had been added (1 mM PMSF, 1 mM leupeptin, 1 mM pepstatin A). The $1,000 \times g$ supernatant was collected, centrifuged at $3,000 \times g$ for 10 min at 4°C , and the resulting pellet washed twice leading to the $3,000 \times g$ membrane fraction. A similar procedure was used to prepare the $6,000 \times g$ and $17,000 \times g$ fractions of subcellular membranes. The preparation of the outer mitochondrial membrane (OMM) and mitoplasts was performed by using the detergent approach described by Ragan *et al.* (18). Briefly, digitonin (Calbiochem) was added to a suspension of 1,000, 3,000, or $6,000 \times g$ mitochondria (100 mg of protein/ml) to a final concentration of 0.6% w/v in isolation medium and incubated for 15 min on ice under gentle stirring. After dilution with 3 volumes of isolation medium, the suspension was centrifuged at $15,000 \times g$ for 10 min at 5°C . The resulting pellet (mitoplasts) was saved, whereas the supernatant was centrifuged at $144,000 \times g$ for 20 min at 5°C leading to a pellet (outer mitochondrial membrane fraction), which was then washed twice. The protein concentration was assayed by the Lowry method. The relative purity of the outer membrane and mitoplasts was assessed from the specific activity of marker enzymes (monoamine oxidase and malate dehydrogenase for the outer membrane and mitoplasts, respectively) as described previously by Ragan *et al.* (18). All chemicals used for the preparations except digitonin were from the Sigma.

Inner Mitochondrial Membrane Vesicle Preparation—The IMM vesicles were prepared as reported previously (18) from the 1,000, 3,000, or $6,000 \times g$ subpopulation of rat liver mitochondria suspended at a protein concentration of 100 mg/ml. Briefly, mitoplasts were prepared as above and resuspended in isolation medium at a protein concentration of 15 mg/ml before being sonicated with a probe sonicator (Vibra-Cell, Sonics & Materials Inc., Berlin, Germany) for six 5-s bursts at the maximum energy setting with 30-s cooling periods. After sonication, mitoplasts were diluted with an equal volume of isolation medium and centrifuged at $15,000 \times g$ for 10 min at 5°C . The resulting pellet was resuspended in 10 volumes of isolation medium and centrifuged again at $100,000 \times g$; this process was repeated twice. The final pellet was resuspended in isolation medium to which protease inhibitors had been added and assayed for its protein content. The purity of the vesicles was assessed by assaying the cytochrome *c* oxidase. The diameter of the IMM vesicles was determined both by a particle size analyzer and by electron microscopy (see below).

Immunoblotting Analysis—Aliquots (60 μg of proteins) of isolated mitochondria, outer membrane, or mitoplasts prepared as above were heated to 90°C and electrophoresed in an SDS, 13% acrylamide gel (Mighty Small II, Amersham Biosciences) using a low molecular weight protein ladder (Amersham Biosciences, Buckinghamshire, UK). The resolved proteins were transferred electrophoretically onto nylon membranes that were blocked in 5% (w/v) low fat milk in blocking buffer (20 mM Tris-HCl, 0.15 M NaCl, 1% Triton X-100, pH 7.5) for 1 h, and further incubated with an affinity-purified rabbit antibody directed against an N-terminal peptide of rat AQP8 (10), AQP9 (Alpha Diagnostics International, San Antonio, TX), or prohibitin (Abcam, Cambridge, UK) all at a final concentration of 1 $\mu\text{g}/\text{ml}$ blocking solution. Horseradish peroxidase anti-rabbit IgG-treated membranes (anti-rabbit IgG peroxidase antibody, Sigma) were developed by luminal-chemiluminescence (ECL-Plus, Amersham Biosciences).

Immunohistochemistry—After being removed, samples of liver were quickly processed to be included in a hydrophilic resin (Technovit 8100, Heraeus-Kulzer, Wehrheim, Germany). Samples were fixed with 4% paraformaldehyde in 0.1 mol/liter phosphate-buffered saline (PBS), pH 7.4, for 4 h at 4°C . After overnight incubation in PBS to which 6.8% sucrose had been added, the samples were then dehydrated with acetone and embedded in Technovit 8100 at 4°C . Before staining, semithin sections were incubated for 5 min at 37°C in 0.01% trypsin in 0.1% CaCl_2 , pH 7.8. AQP8 was localized by the peroxidase-antiperoxidase method. Endogenous peroxidase was blocked by 1% H_2O_2 for 10 min at room temperature. Sections were then incubated overnight at 4°C with the AQP8 affinity-purified antibodies at a final concentration of 5 $\mu\text{g}/\text{ml}$ in blocking buffer (1% normal goat serum in PBS). Successively, sections were treated for 1 h at room temperature with goat anti-rabbit immunoglobulin G (Sigma) diluted 1:100 in blocking buffer and then incubated with peroxidase-antiperoxidase (Sigma) at a dilution of 1:100 for 1 h at room temperature. Finally, the immunolabeling was revealed by incubation with 3,3'-diaminobenzidine/ H_2O_2 medium for 10 min at room temperature. Controls were performed by omitting the primary antibodies.

Immunogold Electron Microscopy—Four animals were used for the study. Samples of liver or testis or mitochondrial pellets were fixed in a

mixture of 3% paraformaldehyde and 1% glutaraldehyde in 0.1 mol/liter PBS at pH 7.4 for 4 h at 4°C . Some specimens were postfixed in 1% OsO_4 in PBS for 30 min at 4°C . Fixed specimens were dehydrated in ethanol and then embedded in Epon (TAAB, Reading, England). Ultrathin sections were mounted on gold mesh grids. Sections of osmicated samples were oxidized with sodium metaperiodate to restore specific labeling. Both osmicated and non-osmicated sections were treated with 0.05 mol/liter glycine in PBS buffer for 15 min at room temperature. Grids were incubated for 30 min at room temperature with 1% bovine serum albumin in PBS containing 0.2% gelatin and then placed on a drop of a solution of the AQP8 N terminus antibody (10 $\mu\text{g}/\text{ml}$ PBS containing 0.2% gelatin) and incubated overnight at 4°C . The grids were then incubated in 1:10 10-nm gold-conjugated anti-rabbit immunoglobulin G (Sigma) in PBS containing 0.2% gelatin for 1 h at room temperature and lightly stained with uranyl acetate and lead citrate. Finally, the grids were observed using a Zeiss EM 109 electron microscope (Zeiss, Oberkochen, Germany). Immunolabeling controls were performed by omitting the AQP8 antibody or using an antibody directed against AQP9. Ten to fifteen images were obtained from each animal or pellet ($1,000 \times g$ fraction) of freshly isolated mitochondria, while morphometric analyses were performed by counting the number of immunogold particles over an overall micrograph surface of about $2,000 \mu\text{m}^2$.

Stopped-flow Light Scattering—The size of the IMM vesicles ($1,000 \times g$ fraction) to be used for the stopped-flow measurements was determined both with a N5 submicron particle size analyzer (Beckman Coulter Inc., Palo Alto, CA) and by morphometric analysis of electron micrographs. The time course of vesicular volume change was followed from changes in intensity of scattered light at the wavelength of 450 nm using a Jasco FP-6200 (Jasco, Tokyo, Japan) stopped-flow reaction analyzer that has a 1.6-ms dead time and 99% mixing efficiency in <1 ms. The sample temperature was controlled by a circulating water bath. To perform the experiments, 35 μl of a concentrated vesicle suspension was diluted into 2.5 ml of a hypotonic (220 mosM) isolation medium (124 mM mannitol, 70 mM sucrose, 20 mM Tris-HCl, 1 mM EDTA, and 5 mM EGTA, pH 7.4). One of the syringes of the stopped-flow apparatus was filled with the vesicle suspension, whereas the other was filled with the same buffer added of mannitol to reach a final osmolarity of 500 mosM to establish a hypertonic gradient (140 mosM) upon mixing. The final protein concentration after mixing was 100 $\mu\text{g}/\text{ml}$. Immediately, after applying a hypertonic gradient, water outflow occurs, and the vesicles shrink, causing an increase in scattered light intensity. The data were fitted to a single exponential function. The osmotic water permeability coefficient (P_f), an index reflecting the osmotic water permeability of the vesicular membrane, was calculated as described (19), using the equation: $P_f = K_{\exp} \cdot V_o / A_v \cdot V_w \cdot \Delta C$, where K_{\exp} is the fitted exponential rate constant, V_o is the initial mean of vesicle volume, A_v is the mean vesicle surface, V_w is the molar volume of water, and ΔC is the osmotic gradient. The medium osmolarity was verified by freezing point depression, using a Halbmikro-Osmometer (Knauer, Berlin, Germany). In some experiments, IMM vesicles were incubated for 5 min in isolation medium deprived of EGTA and EDTA and containing 300 μM HgCl_2 , a sulphydryl compound known to block mammalian aquaporins including AQP8 (20). In other experiments, to verify the blocking action of the Hg^{2+} ion, the HgCl_2 treatment of the vesicles was followed by a 15 min exposure to 10 mM of the reducing agent β -mercaptoethanol. The temperature dependence of osmotic water permeability in the IMM vesicles in the presence or absence of Hg^{2+} inhibition was assessed by determining the activation energy of Arrhenius (E_a) calculated measuring the P_f of the vesicles at 10, 20, and 30°C .

RESULTS AND DISCUSSION

As a first step, we defined the precise subcellular localization of AQP8 in rat liver. This was done by immunohistochemistry and immunoblotting using an affinity-purified immunoglobulin G specific for the rat AQP8 polypeptide. Strong immunohistochemical AQP8 reactivity was seen within the hepatocyte cell interior (Fig. 1A). Overall, AQP8 labeling was found to be greater in the periportal and midlobular than pericentral regions of the hepatic lobule, although hepatocytes with heavy immunostaining were sometimes found in the pericentral region (Fig. 1A, red block arrows). For the immunoblotting experiments, the AQP8 antibody was incubated with fractions of rat liver membranes prepared at different gravitational forces as reported previously (21). A band of expected size, 28 kDa, was strongly detected in the 1,000 and $3,000 \times g$ fractions and,

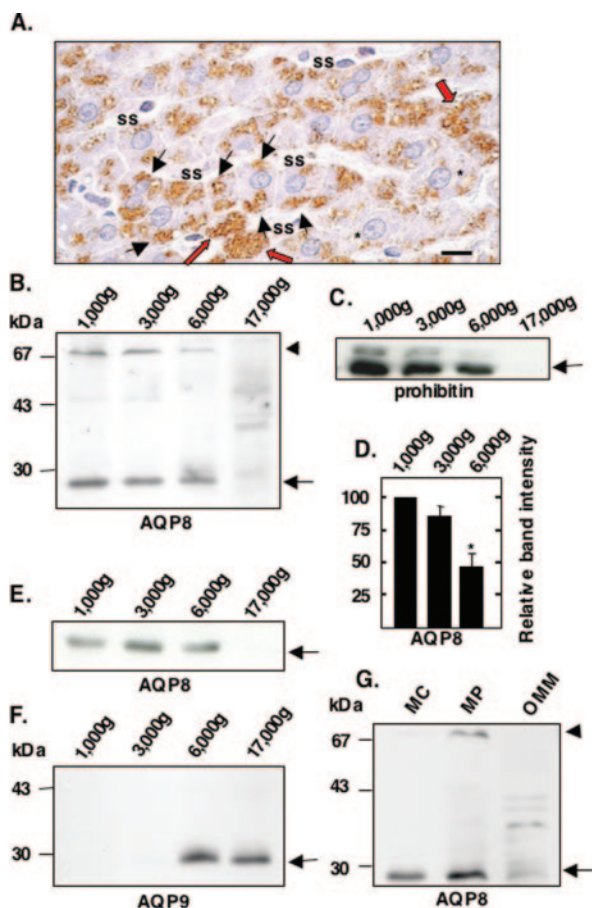


Fig. 1. Analysis of the subcellular and submitochondrial localization of AQP8 in rat liver. *A*, immunohistochemical distribution of AQP8 in liver. Staining is seen in most hepatocytes where intracellular AQP8 often faces the sinusoidal space of Disse (*ss*; *arrows*). Overall, immunoreactivity seems not to be homogeneously distributed among reactive hepatocytes as the extent of the staining ranges between a nearly appreciable one (*asterisks*) and one of extraordinary extension (*red block arrows*). Bar, 20 μ m. *B*, immunoblotting of subcellular membranes of rat liver incubated with an antibody directed against a N terminus AQP8 peptide reveals a strong band of 28 (*arrow*) kDa and another of minor intensity of 75 kDa (*arrowhead*) in the 1,000, 3,000, and 6,000 \times g, fractions which are basically composed of heavy mitochondria. Weak immunoreactivity was detected in the 17,000 \times g pellet, a fraction enriched in plasma membranes. *C*, immunoblotting of liver subcellular membranes incubated with antibodies against prohibitin (*arrow*), a 30-kDa mitochondrial marker protein expressed in the IMM. No apparent reactivity is seen in the plasma membrane fraction (17,000 \times g). *D*, densitometric analysis of the 28 kDa band normalized against the different percentage of mitochondria characterizing the 1,000, 3,000, and 6,000 \times g pellets shows a direct correlation between AQP8 immunoreactivity and mitochondria size. *E*, immunoblotting showing the AQP8 immunoreactivity (28-kDa band; *arrow*) in rat kidney subcellular membrane fractions. *F*, control immunoblotting experiment showing the presence of AQP9 (*arrow*), the basolateral membrane aquaporin of rat hepatocyte, in the 6,000 and 17,000 \times g membrane fractions. *G*, immunoblotting of mitoplasts (MP) and OMM (prepared from 1,000 \times g mitochondria) incubated with the AQP8 antibody. The 28 (*arrow*)- and 75 (*arrowhead*)-kDa bands are stronger in mitoplasts than whole mitochondria (MC). Minor immunoreactive bands can be seen in the outer membrane fraction.

to a lesser extent, in the 6,000 \times g pellet (Fig. 1*B*). An additional band of higher molecular mass was seen in the mitochondrial fraction, likely representing a multimeric form of AQP8 (Fig. 1*B*). Consistent with a previous report (21), microscopic analysis revealed that the 1,000, 3,000, and 6,000 \times g pellets of liver used throughout the experiments were basically composed of mitochondria (98, 96, and 84% of the pellet volume, respectively). This was also confirmed by immunoblotting using antibodies against prohibitin, a mitochondrial marker (Fig. 1*C*).

Supporting a predominant expression of AQP8 in intracellular organelles, the 28-kDa band was very weak in the plasma membrane-enriched fraction (17,000 \times g) (Fig. 1*B*). Interestingly, after normalizing for the different percentage of mitochondria composing the gravitational pellets, densitometric analysis of the above immunoblots showed that the heavier the mitochondrial fraction the stronger the intensity of the 28-kDa band (Fig. 1*D*). By electron microscopy analysis, the average mitochondria size in the 1,000 \times g liver fraction was almost twice and three times larger than the 3,000 and 6,000 \times g fractions, respectively (1.18 ± 0.4 , 0.68 ± 0.4 , and 0.45 ± 0.3 μ m, respectively). Suggesting a wide expression in mitochondria, AQP8 immunoreactivity was detected in the mitochondrial fractions of kidney (Fig. 1*E*) and many other rat organs known to express such AQP including testis, heart, duodenum, jejunum, and colon (data not shown). AQP8 was apparently absent in epididymal spermatozoa (data not shown). Control immunoblotting using antibodies against AQP9, an aquaporin reported to be expressed only in the hepatocyte sinusoidal membrane (22), showed the absence of immunoreactivity in the mitochondrial fractions, while a band of expected molecular mass, 29 kDa, was detected in the fractions containing plasma membrane (Fig. 1*F*). Localization of AQP8 in the inner mitochondrial membrane was indicated by immunoblotting experiments showing higher AQP8 immunoreactivity in mitoplasts than whole mitochondria and negligible staining in the OMM (Fig. 1*G*). This finding was fully consistent with studies of immunogold electron microscopy with both *in situ* and freshly isolated mitochondria, in both cases showing AQP8 immunoreactivity in the IMM and, occasionally, the matrix compartment (Fig. 2, *A*, *B*, and *D*). No distinctive labeling was observed in the OMM when this membrane was clearly visible (Fig. 2*D*). Morphometric analysis of freshly isolated mitochondria (Fig. 2*F*) showed variable AQP8 reactivity among mitochondria, some of which appeared poorly labeled or even unreactive. This pattern of distribution is consistent with the heterogeneous distribution of AQP8 in liver (Fig. 1*A*) and suggests the existence of subpopulations of mitochondria where AQP8 is not expressed. This possibility is corroborated by the apparent absence of immunogold AQP8 particles in the mitochondria of rat epididymal spermatozoa (data not shown). Interestingly, such mitochondria have the distinctive metabolic feature of not performing the β -oxidation of fatty acids and to use fructose as the only carbon source. Future studies will be addressed to identify the metabolic features of the subpopulations of mitochondria expressing AQP8. Consistent with a possible involvement of AQP8 in rapid increases in mitochondrial volume, swollen mitochondria showed AQP8 immunostaining in their IMM (Fig. 2*C*). Confirming the wide presence of AQP8 in mitochondria, immunogold particles were seen in *in situ* mitochondria of rat testis (Fig. 2*D*). No mitochondrial labeling was seen in control experiments where mitochondria were incubated with antibodies directed against the other hepatocyte aquaporin, AQP9 (data not shown).

Having found the presence of an aquaporin water channel in the IMM, we then decided to characterize the biophysical properties of mitochondrial osmotic water transport. To investigate the reciprocal contribution of the channel-mediated (facilitated diffusion) and lipid bilayer (simple diffusion) pathways to the movement of water through the IMM, we directly assessed osmotic water permeability (P_f) and related activation energy (E_a) of basically pure and homogeneous IMM vesicles by measuring scattered light intensity using stopped-flow spectrophotometry. Mitochondria and mitoplasts could not be used for the IMM P_f calculation as they are of heterogeneous size (Fig. 2, *A-D*) and irregular shape (Fig. 3*A*), respectively. IMM vesicles

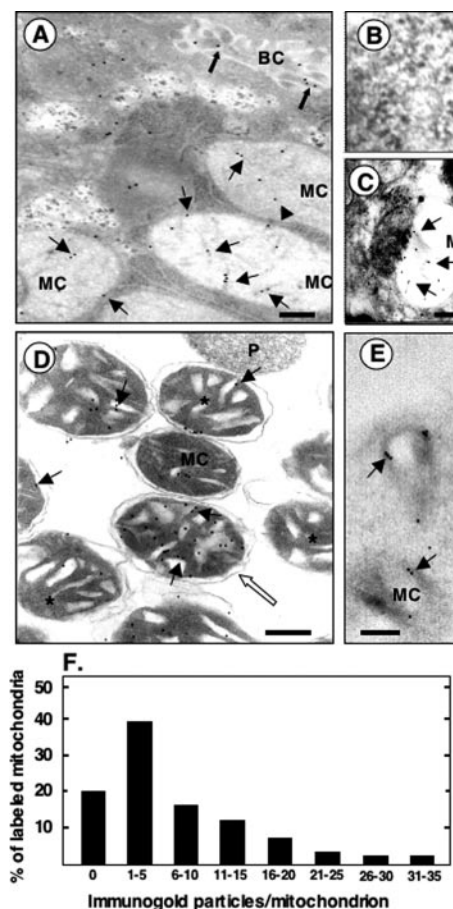


FIG. 2. Submitochondrial localization of AQP8 by immunogold electron microscopy. *A*, *in situ* labeling. AQP8 immunogold particles are seen in mitochondrial cristae and edges (arrows) and, to a much lesser extent, in the matrix compartment (arrowheads). Some labeling is also seen in canalicular microvilli (block arrows). *B*, *in situ* labeling. High magnification micrograph showing immunoreactive AQP8 in the IMM (cristae and border; arrows) and matrix (arrowhead) compartments of the mitochondrion. *C*, *in situ* labeling. Swollen mitochondrion showing AQP8 labeling (arrows). *D*, freshly isolated mitochondria ($1,000 \times g$ fraction). AQP8 staining is seen in the IMM (arrows) and in the matrix subcompartment (arrowheads). AQP8 labeling appears not to be homogeneous among mitochondria as some of them display weak immunoreactivity (asterisks), whereas others are intensely stained (empty block arrow). *E*, *in situ* labeling of rat testis mitochondria. Immunogold particles are seen in mitochondria. *F*, morphometric analysis of the immunodistribution of AQP8 in pellets of freshly isolated mitochondria. BC, bile canaliculus; MC, mitochondrion; P, peroxisome. Bars, 300 nm.

from the $1,000$, $3,000$, or $6,000 \times g$ subpopulations of intact mitochondria were obtained by sonication from liver mitoplasts and had a mean vesicle diameter of 234 ± 31 ($n = 626$), 248 ± 36 ($n = 611$), and 243 ± 28 ($n = 676$) nm, respectively (Fig. 3B). Vesicles were subjected rapidly to a hypertonic osmotic gradient (140 mosm), and the time course of the vesicle shrinkage was followed from the change in scattered light. The osmotic water permeability of all three subpopulations of IMM vesicles was strikingly high (Fig. 3, *C* and *D*) in line with the rapid changes in volume which mitochondria undergo during metabolic homeostasis (23). The highest values of P_f were obtained with the IMM vesicles prepared from the heaviest mitochondria, since the P_f values were of 524.5 ± 6.7 , 496.6 ± 9.0 , and 341.4 ± 4.5 $\mu\text{m/s}$ for the $1,000$, $3,000$, and $6,000 \times g$ fraction, respectively (Fig. 3D). Interestingly, the P_f values paralleled the expression rates of AQP8 in the same mitochondrial populations from which the IMM vesicles were prepared (Fig. 1, *A* and *B*). Proving the absence of mixing artifact, no change in

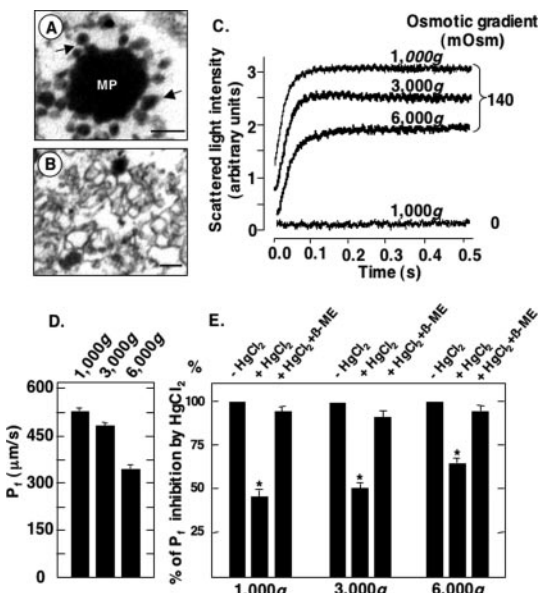


FIG. 3. Biophysical analysis of osmotic water transport across inner mitochondrial membrane vesicles. *A*, electron microscopy showing the irregular shape of liver mitoplasts due to the presence of finger-like projections (arrows). *B*, electron micrograph of a sample of the inner mitochondrial membrane vesicles used for the stopped-flow light scattering studies. *C*, representative experiment of stopped-flow light scattering. A remarkable increase in scattered light (vesicle shrinkage) is observed when IMM vesicles from $1,000$, $3,000$, and $6,000 \times g$ mitochondria are subjected rapidly to a hypertonic osmotic gradient of 140 mosm. No change in scattered light is observed when vesicles are mixed with iso-osmotic buffer (absence of osmotic gradient). *D*, the osmotic membrane water permeability (P_f) of all three IMM vesicle populations is extraordinarily high. The heavier the subpopulation of mitochondria the higher the P_f value of the related IMM vesicles. Data are mean values \pm S.E. from five independent vesicle preparations. *E*, effect of HgCl_2 on the osmotic water permeability of liver IMM. The osmotic membrane water permeability (P_f) of the $1,000$, $3,000$, and $6,000 \times g$ IMM vesicles is significantly reduced by the $300 \mu\text{M} \text{HgCl}_2$ treatment. The HgCl_2 inhibition is reversed by 15-min treatment with $10 \text{ mM} \beta$ -mercaptoethanol. Data are mean values \pm S.E. from five independent vesicle preparations. *, $p < 0.001$. MP, mitoplast. Bars (*A* and *B*), 250 nm.

scattered light was observed when vesicles were mixed with isosmotic buffer (Fig. 3C). Indicating direct correlation between mitochondrial size and importance of the channel-mediated pathway for the water movement across the IMM, the heavier the mitochondrial population the higher the inhibition of the IMM P_f after exposure of the vesicles to $300 \mu\text{M} \text{HgCl}_2$, a known aquaporin blocker acting on the sulphydryl group of a cysteine in the vicinity of the aqueous pore (Cys^{210} in AQP8). The extent of the P_f inhibition of the $1,000$, $3,000$, and $6,000 \times g$ vesicles was $-56.4 \pm 5.2\%$, $-47.6 \pm 3.4\%$, and $-39.6 \pm 4.2\%$, respectively (Fig. 3E). Such inhibitions did not significantly increase when vesicles were exposed both internally and externally to HgCl_2 (data not shown). Consistent with the existence of a Hg^{2+} -inhibitable aqueous pathway for osmotic water permeability across the IMM, the above inhibition was reversed after exposure to the reducing agent β -mercaptoethanol (Fig. 3E). However, the fact that in liver mitochondria we could not detect any reactivity (data not shown) to other known mammalian aquaporins being insensitive to sulphydryl blockers (AQP4 and AQP7) suggests the possible presence of unknown aqueous pores that are insensitive to Hg^{2+} and which provide a non-negligible contribution to the high P_f of the IMM. To examine further the molecular mechanism and pathway(s) of water transport across IMM, we decided to determine the Arrhenius activation energy (E_a) of the osmotic water permeability of the IMM vesicles from temperature dependence data. Some in-

crease in the rate of osmotic water transport was observed when the vesicles were subjected to the same osmotic gradient (140 mosM) at increasing temperatures. Arrhenius plotting of the calculated P_f values at 10, 20, and 30 °C resulted in an E_a of 3.93, 4.51, and 4.93 kcal/mol for the 1,000, 3,000, and 6,000 × g IMM vesicles, respectively. These E_a values, all biophysically consistent with water permeation through aqueous channels (19), showed only slight increases when the IMM vesicles were exposed to HgCl₂ before the stopped-flow light scattering measurements (4.71, 4.86, and 5.11 kcal/mol for the 1,000, 3,000, and 6,000 × g IMM vesicles, respectively). Although the Hg²⁺-inhibitible route accounts for most water permeability of the IMM this result suggests the existence of an additional pathway, a Hg²⁺-insensitive one, facilitating the movement of water across the IMM. The molecular identity of the Hg²⁺-insensitive pathway will be a matter for future investigation.

Mitochondrial AQP8 might act independently or be part of the postulated “permeability transition pore complex” that mediates the rapid entry of solutes and water into the matrix (24, 25), causing swelling of the organelle, rupture of the outer mitochondrial membrane, and release of cytochrome *c* and other key pro-apoptotic elements into the cytoplasm leading to apoptosis. This possibility is corroborated both by the recent observation that treatment with aquaporin blockers prevents the mitoplast swelling induced by the Cd²⁺ ion, a known apoptotic agent (26), and our preliminary studies showing absence of AQP8 in the mitochondrial compartment of immortalized hepatocytes (data not shown). Aquaporins have already been reported to affect the rate of apoptosis by controlling the rate of downstream apoptotic events (27). AQP8 may also be relevant in facilitating the increase in volume which the mitochondrion undergoes when its ATP synthesis efficiency increases because, as seen above, the mitochondria with the highest AQP8 content are also the ones with the greatest diameter (Fig. 1, *B* and *D*), oxidative capacity, and respiratory rate (21, 28). By contrast, AQP8-mediated water movement would not be necessary in small mitochondria performing low oxidative phosphorylation, as sufficient amounts of water can cross the IMM by facilitated diffusion through the unidentified aqueous pore suggested by the above biophysical experiments and by simple diffusion (non-channel mediated pathway). Pathways of simple diffusion through the IMM are 1) the lipid bilayer, which is comparatively large in small mitochondria due to their high surface-to-volume ratio, and 2) the extensive hydrophilic domains created by the extraordinary amount (76%) of proteins composing the IMM.

Overall, as well as biophysically characterizing the osmotic conduit of water across the mitochondrion, we provide biochemical and ultrastructural evidence for the presence of an aquaporin water channel, AQP8, in the inner membrane. Moreover, the existence of a pathway other than aquaporins that facilitates the osmotic movement of water across the IMM is postu-

lated and deserves investigation. AQP8-mediated water movement may be particularly important in the homeostatic control of mitochondrial volume such as in the swelling that the mitochondrion undergoes under apoptotic stimuli and during oxidative phosphorylation. Recognition of AQP8 in mitochondria therefore has profound new implications for an understanding of how mitochondria adapt their morphology.

Acknowledgments—We are grateful to Dr. Peter Agre for his encouragement and valuable suggestions regarding the biophysical studies, W. B. Guggino, Adrian E. Hill, and Raoul A. Marinelli for critical reading of this paper, to Fernando Goglia for his valuable suggestions about mitochondria isolation, and to Anthony Green for proofreading the final text and suggesting stylistic improvements.

REFERENCES

- Garlid, K. D. (1988) in *Mitochondrial Volume Control* (Lemasters, J. J., Hackenbrock, C. R., Thurman, R. G., and Westerhoff, H. V., eds) pp. 259–278, Plenum, New York
- Desagher, S., and Martinou, J. C. (2000) *Trends Cell Biol.* **10**, 369–377
- Ichas, F., Jouaville, L. S., Sidash, S. S., Mazat, J. P., and Holmuhamedov, E. L. (1994) *FEBS Lett.* **348**, 211–215
- Guerrieri, F., Pellecchia, G., Lopriore, B., Papa, S., Liquori, G. E., Ferri, D., Moro, L., Marra, E., and Greco, M. (2002) *Eur. J. Biochem.* **269**, 3304–3312
- Fujii, F., Nodasaka, Y., Nishimura, G., and Tamura, M. (2004) *Brain Res.* **999**, 29–39
- Beavis, A. D., Brannan, R. D., and Garlid, K. D. (1985) *J. Biol. Chem.* **260**, 13424–13433
- Garlid, K. D. (1996) *Biochim. Biophys. Acta* **1275**, 123–126
- Kristián, T., Gertsch, J., Bates, E. T., and Siesjö, B. K. (2000) *J. Neurochem.* **74**, 1999–2009
- Colombini, M. (2004) *Mol. Cell. Biochem.* **256–257**, 107–115
- Palmieri, F. (2004) *Pflügers Arch.* **447**, 689–709
- Agre, P., and Kozono, D. (2003) *FEBS Lett.* **555**, 72–78
- Ferri, D., Mazzone, A., Liquori, G. E., Cassano, G., Svelto, M., and Calamita, G. (2003) *Hepatology* **38**, 947–957
- Gradilone, S. A., Garcia, F., Huebert, R. C., Tietz, P. S., Larocca, M. C., Kierbel, A., Carreras, F. I., LaRusso, N. F., and Marinelli, R. A. (2003) *Hepatology* **37**, 1435–1441
- Portincasa, P., Moschetta, A., Mazzone, A., Palasciano, G., Svelto, M., and Calamita, G. (2003) *J. Hepatol.* **39**, 864–874
- Calamita, G., Mazzone, A., Bizzoca, A., Cavalier, A., Cassano, G., Thomas, D., and Svelto, M. (2001) *Eur. J. Cell Biol.* **80**, 711–719
- Calamita, G., Spalluto, C., Mazzone, A., Rocchi, M., and Svelto, M. (1999) *Cytogenet. Cell Genet.* **85**, 237–241
- Zardoya, R., and Villalba, S. (2001) *J. Mol. Evol.* **52**, 391–404
- Ragan, C. I., Wilson, M. T., Darley-Usmar, V. M., and Lowe, P. N. (1987) in *Mitochondria: A Critical Approach* (Darley-Usmar, V. M., Rickwood, D., and Wilson, M. T., eds) pp. 79–112, IRL Press, Oxford
- van Heeswijk, M. P., and van Os, C. H. (1986) *J. Membr. Biol.* **92**, 183–193
- Ishibashi, K., Kuwahara, M., Kageyama, Y., Tohsaka, A., Marumo, F., and Sasaki, S. (1997) *Biochem. Biophys. Res. Commun.* **237**, 714–718
- Lanni, A., Moreno, M., Lombardi, A., and Goglia, F. (1996) *Int. J. Biochem. Cell Biol.* **28**, 337–343
- Elkjaer, M., Vajda, Z., Nejsum, L. N., Kwon, T., Jensen, U. B., Amiry-Moghaddam, M., Frokiaer, J., and Nielsen, S. (2000) *Biochem. Biophys. Res. Commun.* **276**, 1118–1128
- Bereiter-Hahn, J. (1990) *Int. Rev. Cytol.* **122**, 1–63
- Zoratti, M., and Szabo, I. (1994) *J. Bioenerg. Biomembr.* **26**, 543–553
- Vander Heiden, M. G., Chandel, N. S., Williamson, E. K., Schumacker, P. T., and Thompson, C. B. (1997) *Cell* **91**, 627–637
- Lee, W-K., Bork, U., Gholamrezaei, F., and Thévenod, F. (2005) *Am. J. Physiol.* **288**, F27–F39
- Jablonski, E. M., Webb, A. N., McConnell, N. A., Riley, M. C., and Hughes, F. M. (2004) *Am. J. Physiol.* **286**, C975–C985
- Weibel, E. R., Staubli, W. S., Gnagi, H. R., and Hess, F. A. (1969) *J. Cell Biol.* **42**, 68–85